Solid State Sciences 37 (2014) 103–107

Contents lists available at ScienceDirect

Solid State Sciences

journal homepage: www.elsevier.com/locate/ssscie

Li ion diffusion in $LiAlO_2$ investigated by Raman spectroscopy

Qiwei Hu [a], Li Lei [a, b, *], Xiaodong Jiang [a], Zhe Chuan Feng [c], Mingjun Tang [d], Duanwei He [a, b]

[a] Institute of Atomic and Molecular Physics, Sichuan University, 610065, Chengdu, China
[b] Key Laboratory of High Energy Density Physics and Technology of Ministry of Education, Sichuan University, 610064, Chengdu, China
[c] Graduate Institute of Electro-Optical Engineering and Department of Electrical Engineering, National Taiwan University, Taipei, Taiwan, 106, China
[d] College of Physics and Electronic Engineering, Sichuan Normal University, Chengdu, 610066, China

ARTICLE INFO

Article history:
Received 15 June 2014
Received in revised form
24 August 2014
Accepted 29 August 2014
Available online 9 September 2014

Keywords:
$LiAlO_2$
Raman spectroscopy
Temperature dependence
Li diffusion
Bandwidth

ABSTRACT

The temperature dependence of Li ions behavior of γ-$LiAlO_2$ has been studied from 78 to 873 K. On heating, the Li ions underwent positional disordering along the structural channels, with the Li ions related modes at 220, 366 and 400 cm^{-1} broadening and weakening dramatically. An anomalous maximum in the bandwidths of the Li ions related modes is observed. It should be apparent that there are at least two distinct thermally activated processes. A model suggested by Andrade and Porto is used to describe the linewidth of a phonon.

1. Introduction

The γ-$LiAlO_2$ crystallizes in the tetragonal space group $P4_12_12$. A unit cell contains four formula units and has lattice parameters $a = 0.51687$ nm and $c = 0.62679$ nm [1]. Its crystal structure can be described as a three-dimensional network of LiO_4 and AlO_4 tetrahedron sharing summits and edges [2]. γ-$LiAlO_2$ is used as a coating in Li electrodes and as an additive in composite Li electrolytes [3], in which Li ion diffusion is a crucial process for these applications. Furthermore, γ-$LiAlO_2$ is used as a substrate material for epitaxial growth of III–V semiconductors like GaN [4]. However, the stability of such systems during processing and operation will depend on lithium diffusion in the substrate and from the substrate into the semiconducting films. γ-$LiAlO_2$ is also considered as a candidate material for tritium breeder or fusion reactors [5,6]. In this case, tritium release and diffusion will depend on lithium diffusion in this material.

Therefore, Tarte [7] investigated the vibrational property of γ-$LiAlO_2$ by infra-red spectra and assigned Li and Al related modes with the help of ^6Li–^7Li isotopic shifts. The Li vibrational modes distribute in low frequency region below 500 cm^{-1}. Alessandrini et al. [8] studied the ion conductivity by impedance spectroscopy with increasing temperature. Due to the Li ion diffusion, the "extrinsic" conductivity is occurring even about 200 °C. A molecular dynamics simulation had been carried out, predicting a Li diffusion coefficient of 2.8×10^{-11} m^2/s at 600 K and an activation energy of 0.5 eV [9]. Recently, Indris et al. [10] studied the dynamics of lithium ions in single crystalline γ-$LiAlO_2$, with temperature-dependent ^7Li NMR spectroscopy and conductivity measurements. However, the activation energies of Li ion turned out to be 0.7 eV and 1.26 eV, respectively.

In a word, one of the major problems in the study of γ-$LiAlO_2$ is to understand in some detail the dynamical behavior of the Li ion. Of particular interest is the effect of the potential-energy environment of the crystal on the motion of the Li ion. A temperature-dependent vibrational spectroscopic study can provide information about not only the potential-energy environment of the mobile ion but also information concerning dynamical processes in the crystal which are coupled to the ionic motion and affect the behavior of the ion. In this study, we present investigations of the vibrational properties of γ-$LiAlO_2$ both theoretically, though *ab initio* calculation, and experimentally, though Raman scattering at temperature from 78 to 873 K. The temperature dependence of the bandwidth of Li ion vibrational modes in γ-$LiAlO_2$ is particularly interesting and is the focus of this paper.

* Corresponding author. Institute of Atomic and Molecular Physics, Sichuan University, 610065, Chengdu, China.
E-mail address: lei@scu.edu.cn (L. Lei).

http://dx.doi.org/10.1016/j.solidstatesciences.2014.08.017
1293-2558/

2. Experiments and calculations

The γ-$LiAlO_2$ was synthesized by the conventional solid-state reaction method from high-purity α-Al_2O_3(99.99%) and Li_2CO_3(99.99%) powders which were mixed at the stoichiometric molar ratio 1:1 and sintered subsequently. The as-prepared samples were identified and characterized by powder X-ray diffraction ($\lambda_{Cu} = 1.54056$ Å, Fangyuan DX-2500, China) at 0.03°/s steps over the range of $2\theta = 10–100°$) at room temperature.

The confocal micro-Raman scattering measurements were carried out in the backscattering geometry based on triple grating monochromator (Andor Shamrock SR-303i-B, EU) with an attached EMCCD (ANDOR Newton DU970P-UVB, EU), excitation by a solid-state laser at 532 nm (RGB lasersystem, NovaPro, Germany), and collection by a 100X, 0.90 NA objective (Olympus, Japan). The output power of the 532 nm laser was fixed to 20 mW and the laser power on the sample surface is about 5 mW. The Raman shifts were carefully calibrated using Si plate with an uncertainty of 0.5 cm^{-1}.

Low and high temperature experiments were performed with mounting the sample on the Linkam Heating and Freezing Stage (THMS600, UK), where the temperature could be varied from 78 to 873 K by introducing liquid nitrogen.

The first-principle calculations were performed with the *CASTEP* code based on DFT [11]. The norm-conserving pseudo-potential with the same cutoff energy of 800 eV was used to describe the interaction between electrons and ions. The local-density approximation (LDA) was adopted to describe the exchange and correlation potentials for electron–electron interaction [12]. During the subsequent calculations, the difference in total energy is minimized to below 5×10^6 eV/atom, the maximum ionic Hellmann–Feynman force is converged to less than 0.001 eV/Å, and the total stress tensor is reduced to the order of 0.002 GPa by using the finite basis-set corrections. Integrations in Brillouin zone are performed using special *k* points generated with $6 \times 6 \times 6$ and $3 \times 2 \times 3$ mesh parameters grid.

3. Results and discussion

3.1. Vibrational-mode assignments in γ-$LiAlO_2$

After subtraction of two acoustic modes, the vibrational modes at the Γ point are distributed among the following irreducible representations: $\Gamma = 12E(R; IR) + 7A_2(IR) + 7B_2(R) + 5B_1(R) + 5A_1(R)$. The A_1 mode and B mode are non-polar Raman active (R) modes while the E modes are polar Raman and infrared (IR) modes.

The room Raman spectra are presented in Fig. 1. Although assigning all the individual vibrational modes of γ-$LiAlO_2$ appears difficult or even impossible at this stage, the observed signals can be tentatively divided into two regions: the low- and high-frequency ones, below and above 500 cm^{-1}, respectively. According to Tarte [7], the high-frequency region mainly involves the vibration of Al–O while the low-frequency mainly Li–O and the mixture of Li–O and Al–O. Furthermore, in other Li-based compounds such as $LiAlSiO_4$, Handke et al. [13] assigned the modes near 246 and 300 cm^{-1} as Li–O stretching as these bands showed isotope shifts of 8.7 and 10.6 cm^{-1}, respectively, through $^6Li/^7Li$ isotope substitution. With the help of the *ab initio* calculation, a summary of the mode frequencies and various assignments are presented in Table 1. The modes at 220, 366 and 400 cm^{-1} are assigned as Li–O stretching motion and the modes at 123, 260 and 268 cm^{-1} as LiO_4–AlO_4 and Li–O–Al vibration, respectively.

3.2. Temperature dependence of Raman spectroscopy of γ-$LiAlO_2$

Temperature dependent Raman spectra measured from 78 to 873 K are shown in Fig. 2a, b. The effect of increasing temperature

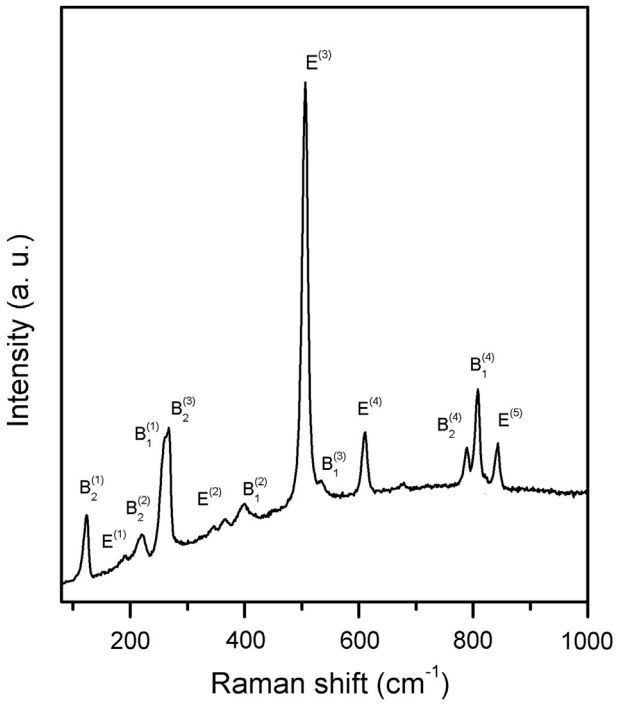

Fig. 1. Raman spectrum of γ-$LiAlO_2$ in room temperature.

can be seen as an increase in band width, a decrease in band intensity and a shift in phonon frequency. The $B_2^{(2)}$ mode at 220 cm^{-1}, the $E^{(2)}$ mode at 366 cm^{-1} and the $B_1^{(2)}$ mode at 400 cm^{-1} started to broaden even at 253 K and then show dramatic decrease in intensity and increase in width upon further heating (Fig. 2a). They become essentially undetectable above 573 K, while a new band appears unexpectedly near 346 cm^{-1}. This behavior can be attributed to positional disordering of Li ions along the structural channels, as was revealed by the previous diffraction studies [14,15]. Similar spectroscopic observations of thermally induced Li disorder have been reported in other Li-based compounds in nearly the same spectral regions [16,17]. The frequencies of these modes decrease with increasing temperature (Fig. 3). It is interesting to note that the $B_1^{(1)}$ mode at 260 cm^{-1} and the $B_2^{(3)}$ mode at 268 cm^{-1} show a splitting behavior. At low temperature, the $B_1^{(1)}$ mode dominates the band. As the temperature increases, the $B_2^{(3)}$ mode becomes stronger and dominates the band above 373 K. The complex variation in the features of these bands implies that the Al–O framework may distort in response to the Li ions positional

Table 1
Observed Raman modes of γ-$LiAlO_2$ and tentative mode assignments. ω_{exp} and ω_{calc} are the frequencies of experiment and calculation (in units of cm^{-1}), respectively.

Raman mode	Mode description	ω_{exp} (cm^{-1})	ω_{calc} (cm^{-1})
$B_2^{(1)}$	LiO_4–AlO_4	124	117
$E^{(1)}$	Li–O–Al bending	187	185
$B_2^{(2)}$	Li–O stretching	220	230
$B_1^{(1)}$	Li–O–Al stretching	260	270
$B_2^{(3)}$	Li–O–Al stretching	268	278
$E^{(2)}$	Li–O bending	366	382
$B_1^{(2)}$	Li–O stretching	398	388
$E^{(3)}$	Al–O bending	508	494
$B_1^{(3)}$	Al–O stretching	540	530
$E^{(4)}$	Al–O bending	613	625
$B_2^{(4)}$	Al–O stretching	791	737
$B_1^{(4)}$	Al–O stretching	809	793
$E^{(5)}$	Al–O bending	844	799